SOLUTION MINING
RESEARCH INSTITUTE

1745 Chris Court
Deerfield, Illinois 60015-2079
USA
Telephone: 847-374-0490 Fax: 847-374-0491
E-mail: bdiamond@mcs.com

Meeting Paper

A Tentative Classification of Salts According to their Creep Properties

by

P. Bérest
B. Brouard

Laboratoire de Mécanique des Solides
(Centre commun X-Mines-Ponts, U.R.A. 317 du C.N.R.S.)
Ecole Polytechnique
91128 Pallaiseau Cedex
France

Spring 1998 Meeting
New Orleans, Louisiana, USA
April 19-22, 1998

INTRODUCTION

Many laboratory works have been devoted to the rheology of rock-salt. The matter exhibits a fascinating complexity. Together with actual stresses, stress history, temperature and humidity play a significant role. A wide literature is available (for instance, see Hardy and Langer, 1984, 1988; Ghoreychi, Bérest, Hardy and Langer, 1996; Aubertin and Hardy, 1997). Despite this complexity, many authors agree on several main features of rock-salt constitutive behavior:

- First, salt behaves like a fluid in the sense that it flows even under small deviatoric stress. Salt is a non-newtonian fluid and its strain rate is proportional to a rather high power of applied deviatoric stress (which means that the creep rate of a cavern is a highly non-linear function of its internal pressure or, more precisely, of the gap between the lithostatic pressure at cavern depth and its internal pressure).
- The strain rate is also strongly influenced by temperature; enlarging by one or two orders of magnitude when the temperature increases by 100°C, (i.e. 180°F).

This means that cavern depth will influence cavern convergence both through the influence of overburden pressure and through rock mass temperature.

On the other hand, few well-documented field data are available. Some deep natural gas storages have experienced large volume losses; well known cases include the Eminence Salt Dome gas storage in Louisiana (Baar, 1977), the Kiel gas cavern in Germany (Kuhne *et al.*, 1973), and the Tersanne Te02 cavern in France (Boucly, 1982) (see Figure 1). Several shut-in tests or brine flow measurements have been performed in different sites. The results are, in general, heavily influenced by brine thermal expansion (Bérest *et al.*, 1998), where the real effect of creep is hidden by the leading part played by brine temperature variations. We have measured brine outflow in a small 930 meter deep cavern in the Etrez site, several years after the end of leaching, when brine thermal expansion becomes negligible (Brouard, 1998).

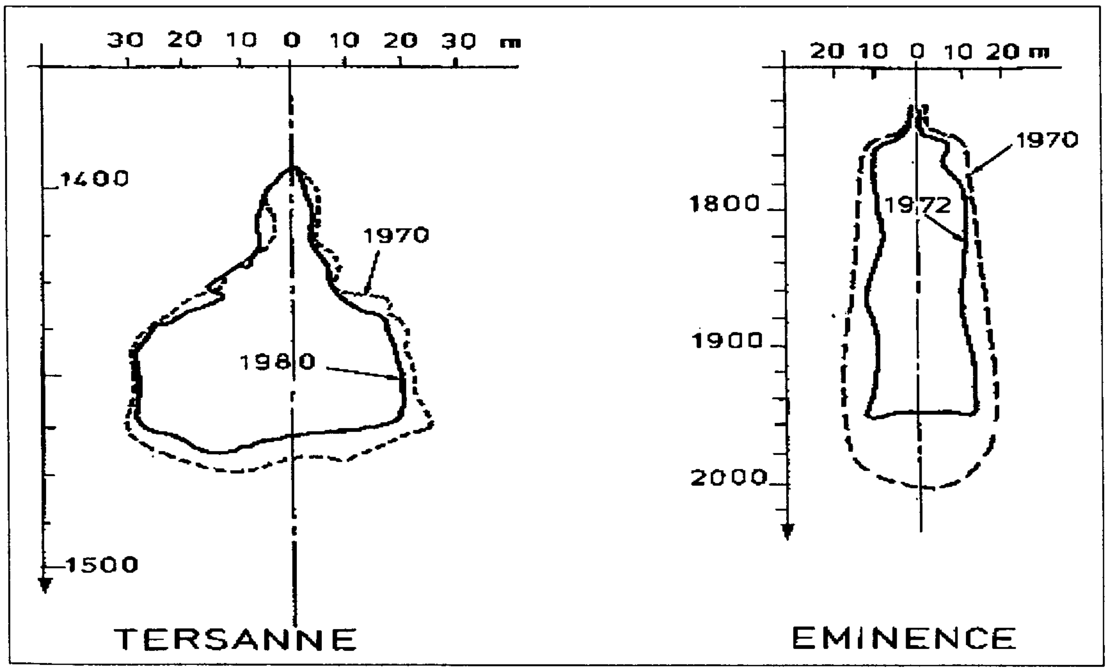

Figure 1: Cavern convergence in Tersanne (Boucly, 1982) and Eminence (Baar, 1977).

One consequence is that althought it is extremely important for a correct understanding of salt mechanical behavior, the efficiency of a sophisticated constitutive law, including finicky details on transient effects or rock temperature variations, can hardly be fully validated by field data, which are often rather rough, when available. From this point of view, numerical computations are far in advance of available field evidence.

From this set of arguments, we find it useful to select a rather simple constitutive model that captures the mean features of salt behavior, and to systematically compute the consequences of the selected set of model parameters on the behavior of salt caverns.

The selected constitutive model has been proposed by many authors, at least as a simplified version of more sophisticated rheological laws. The steady-state (or "secondary") salt creep is described by a Norton-Hoff model, or power law, whose uniaxial formulation can be written as:

$$\dot{\varepsilon} = A \exp\left(-\frac{Q}{RT}\right) \sigma^n$$

where $\dot{\varepsilon}$ is the axial strain rate of a cylindrical sample ($\dot{\varepsilon} = -\dot{h}/h$) submitted to an axial stress, P, and to a lateral confinement pressure, q, whose difference is $\sigma = P - q$.. In other words, during an uniaxial compression test, σ is simply the applied load ($q = 0$). The (absolute) temperature is T, and the three constants ($A, Q/R$ and n) must be determined through laboratory experiments. The case $n = 1$ is described as being "Newtonian": the flow rate is simply proportional to the applied shear stress. Salt rock is definitely not a Newtonian fluid: the constant n ranges from $n = 3$ to $n = 6$ for most cases.

The uniaxial formulation of material constitutive behavior is very convenient for a description of triaxial laboratory test results, but it must be generalized to the three-dimensional case for use in numerical calculations. It is generally assumed that rock salt has no volumetric expansion or contraction, at least prior to failure. Thus, if $\underline{\underline{d}}$ holds for the strain rate tensor, $\underline{\underline{\sigma}}$ is the stress tensor, $\underline{\underline{s}}$ is the deviatoric stress tensor, $s_{ij} = \sigma_{ij} - \mathrm{tr}(\underline{\underline{\sigma}})/3$, and J_2 is the second invariant of the deviatoric stress tensor $J_2 = \frac{1}{2} s_{ij} s_{ji}$, then the salt constitutive behavior can be written as:

$$d_{ij} = \frac{\partial \Phi}{\partial s_{ij}} \quad , \quad \Phi = A \exp\left(-\frac{Q}{RT}\right) \frac{\left(\sqrt{3J_2}\right)^{n+1}}{(n+1)}$$

To what extent such a law captures the main features of the mechanical behavior of salt must be discussed. Elastic properties are not taken into account, nor is transient behavior, which is probably of utmost importance when cavern internal pressure exhibits large and frequent changes (as is certainly the case in natural gas storages). Furthermore, this simplified creep law does not properly cover the whole range of stresses which are experienced by rock salt during a cavern life span; small deviatoric stresses effects, for instance, are probably poorly represented by such an unified constitutive law.

LITERATURE DATA

Parameters for such a constitutive law can be found in the literature. It must be clear that these parameters are not *recommended* by the authors, who, in some cases, suggest more elaborate constitutive equations. Furthermore, in the following we will use these data to compute the theorical behavior of caverns at different depths; in many cases, these computations do not apply to real caverns in real sites, whose depths can be different from the depths selected for illustration.

• The first set of data is provided by Van Sambeek (1993) who compiled De Vries (1988) and Munson *et al.* (1989) data. He selected the following form:

$$\dot{\varepsilon} = A \exp\left(-\frac{Q}{RT}\right) \left(\frac{\sigma}{\mu}\right)^n$$

No	Facility	A (/s)	Q (kcal/mole)	R (cal/mole/K)	n	μ (GPa)
1	Avery Island (a)	1.313 10^9	12.9	1.986	3.14	9.6
2	W.I.P.P.	9.672 10^{12}	10.0	1.986	5.0	12.4

Wawersick (1984) uses the same form of law as Van Sambeek.
The temperatures are between 40°C and 160°C.

No	Facility	A (/s)	Q (kJ/mole)	R (J/mole/K)	n	μ (GPa)
3	Salado WIPP7	7.97 10^{17}	69.18	8.3143	5.09	12.4
4	Asse (after Wawersick)	3.05 10^{22}	82.76	8.3143	6.25	12.4
5	West Hackberry WH1	3.30 10^{14}	54.84	8.3143	4.73	12.4
6	West Hackberry WH2	7.92 10^{12}	89.38	8.3143	4.99	12.4
7	Bryan Mound BM3C	1.61 10^{14}	63.29	8.3143	4.54	12.4
8	Bryan Mound BM4C	5.26 10^{18}	74.53	8.3143	5.18	12.4
9	Bayou Choctaw BC1	8.45 10^{10}	49.45	8.3143	4.06	12.4

- The following authors have proposed a similar form

$$\dot{\varepsilon} = A \exp\left(-\frac{Q}{RT}\right) \sigma^n \qquad , \qquad \sigma \text{ in MPa}$$

Pouya (1991) has studied Etrez salt; Senseny (1984) has studied four different salts, and gives the following *mean* values (the range of temperature is 20°C-200°C):

No	Facility	A (/MPa^n/s)	Q/R (K)	n
10	Etrez	2.03 10^{-8}	4100	3.1
11	Avery Island (b)	0.066 10^{-3}	6565	4.0
12	Salina	8.8 10^{-3}	8715	4.1
13	Palo Duro, unit 4	5.7 10^{-3}	9760	5.6
14	Palo Duro, unit 5	8.0 10^{-3}	9810	5.3

More recently the B.G.R. from Hannover has proposed for the Asse mine salt a slightly different set of parameters (see for instance Heusermann, 1996):

No	Facility	A (/MPa^n/day)	Q (kJ/mole)	R (J/mole/K)	Q/R (K)	n
15	Asse B.G.R.	2.08 10^{-6}	54.	8.3143	6495	5.0

The authors do not use the same units, and we have converted the constants to get years, Megapascal and Kelvin degrees, which are more convenient for the problem we are discussing. Kelvin degrees are convenient, since they avoid the problem of heat units (calorie or Joule). The conversion rules are as follows:

$$T^\star \text{ (K)} = Q/R = 10^3\, Q \text{ (kJ/mole)}/(8.3143) = 10^3\, Q \text{ (kcal/mole)}/(1.986)$$

$$\left\{ \begin{array}{ll} A^\star \text{ (MPa}^{-n}\text{year}^{-1}) = 3.1536\, 10^7\, \mu^{-n} \text{ (MPa}^{-n}) \; A \text{ (s}^{-1}) & [(1) \text{ to } (9)] \\ A^\star \text{ (MPa}^{-n}\text{year}^{-1}) = 3.1536\, 10^7\, A \text{ (MPa}^{-n}\text{s}^{-1}) & [(10) \text{ to } (14)] \\ A^\star \text{ (MPa}^{-n}\text{year}^{-1}) = 365\, A \text{ (MPa}^{-n}\text{day}^{-1}) & [(15)] \end{array} \right.$$

No	Facility	n	$T^\star = Q/R$ (K)	$A^\star$ (year^{-1}.MPa^{-n})
1	Avery Island (after D.V.)	3.14	6495	1.30 10^4
2	WIPP	5.0	5035	1.04
3	Salado (WIPP7)	5.09	8333	3.67 10^4
4	Asse (after W.)	6.25	9969	2.51 10^4
5	West Hackberry (WH1)	4.73	6606	452.31
6	West Hackberry (WH2)	4.99	10766	0.94
7	Bryan Mound (BM3C)	4.54	7623	1.32 10^3
8	Bryan Mound (BM4C)	5.18	8977	1.04 10^5
9	Bayou Choctaw (BC1)	4.06	5956	64.03
10	Etrez	3.1	4100	0.64
11	Avery Island (after S. and al.)	4.0	6565	2081
12	Salina	4.1	8715	2.7752 10^5
13	Palo Duro - Unit 4	5.6	9760	1.806 10^5
14	Palo Duro - Unit 5	5.3	9810	2.52 10^5
15	Asse (B.G.R.)	5.0	6495	65.7

A direct comparison is difficult: the constant $A^\star$ varies in a wide range (typically from 1 to 10^5) but when $A^\star$ is large, $T^\star = Q/R$ is large too, resulting in much less scattered values of the product $A^\star\exp(-T^\star/T)$.

Behavior of spherical and cylindrical caverns

Consider a spherical cavern located at depth H below ground level [which means that the overburden pressure is P_∞ (MPa) $= 0.022\ H$ (meters)]. P_i is the constant cavern fluid pressure [for a brine-filled cavern opened to the atmosphere, we get P_i (MPa) $= 0.012\ H$ (meters)]; its steady-state *relative* volume loss rate is given by

$$\frac{\dot{V}}{V} = -\frac{3}{2}\left[\frac{3}{2n}\left(P_\infty - P_i\right)\right]^n A \exp\left(-\frac{Q}{RT}\right)$$

where $n, A, Q/R$ are as above. A similar formula for a cylindrical cavern has been given by Van Sambeek (1993) (these two solutions have also been discussed by Prij, 1991):

$$\frac{\dot{V}}{V} = -\sqrt{3}\left[\frac{\sqrt{3}}{n}\left(P_\infty - P_i\right)\right]^n A \exp\left(-\frac{Q}{RT}\right)$$

which means that the cylindrical case can be deduced from the spherical case by multiplying the former formula by $(2/\sqrt{3})^{n+1}$. Between all possible shapes, the slowest rate is reached when the cavern is spherical.

Three comments must be added:

- These formula are not very different from the formulas given for uniaxial strain rate. The difference $(P_\infty - P_i)$ plays the same role as the applied stress σ.
- Real caverns are neither spherical nor perfectly cylindrical; a flat cavern (i.e. having a diameter much larger than its height) behaves fairly distinctly, as is quite clear in the case of a purely elastic behavior (Bérest *et al.*, 1997). Analysis of the influence of the cavern shape would justify another paper. The spherical/cylindrical cases provide a good illustration of most caverns of regular shape.

- Even when salt behavior is assumed to be steady-state (elastic and transient parts of the mechanical behavior are neglected), the cavern behavior, when submitted to a constant internal pressure lower than lithostatic pressure after time $t = 0$, reaches a steady-state regime but only after a relatively long period of time, due to rearrangement of the stress distribution in the rock mass from its initial homogeneous value to the final steady-state distribution.

In order to make comparisons easier, we will rewrite the former expressions as follows

$$\frac{\dot{V}}{V} = -\dot{\varepsilon}_{1000} \left(\frac{P_\infty - P_i}{P_o}\right)^n \exp\left(\frac{Q}{RT_o} - \frac{Q}{RT}\right)$$

where $T_o = 315$ K and $P_o = 10$ MPa are fixed temperature and pressure that are selected in order that $\dot{\varepsilon}_{1000}$ is the cavern volume rate loss calculated for a 1000 meters deep cavern whose internal pressure is $P_i = 12$ MPa (this is the pressure of a brine-filled cavern opened to the atmosphere), the rock temperature at cavern depth being selected as 315 K, or 42°C, or 108°F.

For a spherical cavern

$$\dot{\varepsilon}^{sph}_{1000} = \frac{3}{2}\left(\frac{3}{2n}\right)^n A\, P_o^n \exp\left(-\frac{Q}{RT_o}\right)$$

For a cylindrical cavern

$$\dot{\varepsilon}^{cyl}_{1000} = \left(\frac{2}{\sqrt{3}}\right)^{n+1} \dot{\varepsilon}^{sph}_{1000}$$

No	Facility	n	Q/R (K)	$\dot{\varepsilon}^{sph}_{1000}$ (10^{-2}/year)	cylinder/sphere ratio	$\dot{\varepsilon}^{cyl}_{1000}$ (10^{-2}/year)
1	Avery Island (after D.V.)	3.14	6495	0.29	1.81	0.53
2	WIPP	5.0	5035	0.0043	2.37	0.01
3	Salado (WIPP7)	5.09	8333	0.0044	2.40	0.011
4	Asse (after W.)	6.25	9969	0.000016	2.84	0.000046
5	West Hackberry (WH1)	4.73	6606	0.012	2.28	0.028
6	West Hackberry (WH2)	4.99	10766	$5\ 10^{-11}$	2.37	$1.2\ 10^{-10}$
7	Bryan Mound (BM3C)	4.54	7623	0.0014	2.22	0.0031
8	Bryan Mound (BM4C)	5.18	8977	0.0016	2.43	0.0039
9	Bayou Choctaw (BC1)	4.06	5956	0.012	2.07	0.025
10	Etrez	3.1	4100	0.028	1.80	0.051
11	Avery Island (after S. and al.)	4.0	6565	0.055	2.05	0.11
12	Salina	4.1	8715	0.0082	2.08	0.017
13	Palo Duro - Unit 4	5.6	9760	0.00024	2.58	0.00061
14	Palo Duro - Unit 5	5.3	9810	0.00028	2.47	0.00069
15	Asse (B.G.R.)	5.0	6495	0.0027	2.37	0.0063

Table 1: Steady-state convergence rate of a brine-filled spherical or cylindrical cavern opened to the atmosphere and located at a 1000 meters depth where the temperature is assumed to be 42°C (108°F).

Cavern convergence for a brine-filled 1000-meter deep cavern varies from $5\ 10^{-11}\%$ year^{-1} (West Hackberry WH2) to 0.29% (Avery Island - after D.V.). It must be kept in mind that these values are calculated from laboratory experiments data. For instance, the calculated value for Etrez salt is 0.028% per year in the spherical case, which appears quite similar to the results of several in situ tests (Brouard, 1998). which proved that the field creep rate in a 930-meter deep cavern was 0.025-0.03% per year.

Large discrepancies can be explained by poor sampling or scale effect. Furthermore, the parameter fitting often covers a wide range of temperatures (the reason is that in many cases the primary concern of these tests was nuclear waste disposal, in which temperatures as high as 200°C must be considered). Then the parameter fitting gives a large importance to tests performed at much higher temperatures than those encountered in standard storage caverns, and may be poorly adapted to our purpose. This can explain some very low convergence rate figures.

No	Facility	n	Q/R (K)	$\dot{\varepsilon}^{sph}_{1500}$ (10^{-2}/year)	cylinder/sphere ratio	$\dot{\varepsilon}^{cyl}_{1500}$ (10^{-2}/year)
1	Avery Island (after D.V.)	3.14	6495	2.68	1.81	4.86
2	WIPP	5.0	5035	0.068	2.37	0.161
3	Salado (WIPP7)	5.09	8333	0.115	2.40	0.275
4	Asse (after W.)	6.25	9969	0.001	2.84	0.002
5	West Hackberry (WH1)	4.73	6606	0.22	2.28	0.50
6	West Hackberry (WH2)	4.99	10766	$2\ 10^{-9}$	2.37	$4\ 10^{-9}$
7	Bryan Mound (BM3C)	4.54	7623	0.026	2.22	0.058
8	Bryan Mound (BM4C)	5.18	8977	0.048	2.43	0.117
9	Bayou Choctaw (BC1)	4.06	5956	0.146	2.07	0.302
10	Etrez	3.1	4100	0.18	1.80	0.32
11	Avery Island (after S. and al.)	4.0	6565	0.71	2.05	1.47
12	Salina	4.1	8715	0.15	2.08	0.32
13	Palo Duro - Unit 4	5.6	9760	0.009	2.58	0.024
14	Palo Duro - Unit 5	5.3	9810	0.010	2.47	0.024
15	Asse (B.G.R.)	5.0	6495	0.052	2.37	0.122

Table 2: Steady-state convergence rate of a brine-filled spherical or cylindrical cavern opened to the atmosphere and located at a 1500 meters depth where the temperature is assumed to be 57°C (135°F).

Tables 1 and 2 give an illustration of depth effect. In the two cases, overburden pressure and cavern pressure are a linear function of depth (P_∞ (MPa) $= 0.022\,H$ (meters) and P_i (MPa) $= 0.012\,H$ (meters) respectively).

Temperature is assumed to vary with depth according to the formula $T(°\mathrm{C}) = 12 + 0.03\,H$ (meters).

Behavior of a natural gas caverns at low pressure

In liquid-filled caverns, the gap between overburden pressure and cavern pressure is more-or-less a linear function of depth

$$P_\infty - P_i \text{ (MPa)} = 0.01\ H \text{ (meters)}$$

Things are quite different in natural gas caverns, where the internal pressure (P_i) varies in a wide range. The minimum gas pressure is often fixed by the gas transportation system pressure. The maximum gas pressure is selected to prevent gas leak through the cemented casing and casing shoe. A typical maximum value is P_{max} (MPa) $= 0.019\,H$ (meters).

Creep is most severe when internal pressure is low. We have selected a minimum pressure, $P_i^{min} = 8$ MPa for a 1500-meter deep cavern. The overburden pressure [$P_\infty = 0.022\,H = 33$ MPa] and the rock-mass temperature distribution [$T = 12 + 0.03\,H = 57°$C] are as assumed above.

It must be noted that the computed volume loss rates give a rough estimation of the real behavior of a cavern, for constant pressure and steady-state creep are assumed; in real world, cavern gas pressure significantly changes one or several times a year, and a precise computation needs for more elaborate computing devices. The main interest of the presented calculations is to outline the drastic effect of low pressures in the cavern.

In the Tersanne case, quoted above, the measured average convergence rate for ten years was $3\ 10^{-2}$ per year (but the cavern was submitted to the minimal pressure during small periods of time). Tersanne salt creep appears much higher than average computed values, which is consistent with laboratory tests performed on Tersanne salt.

No	Facility	n	Q/R (K)	$\dot{\varepsilon}^{sph}_{1500}$ (10^{-2}/year)	cylinder/sphere ratio	$\dot{\varepsilon}^{cyl}_{1500}$ (10^{-2}/year)
1	Avery Island (after D.V.)	3.14	6495	13.3	1.81	24.2
2	WIPP	5.0	5035	0.875	2.37	2.075
3	Salado (WIPP7)	5.09	8333	1.55	2.40	3.71
4	Asse (after W.)	6.25	9969	0.021	2.84	0.059
5	West Hackberry (WH1)	4.73	6606	2.46	2.28	5.61
6	West Hackberry (WH2)	4.99	10766	$2\ 10^{-8}$	2.37	$5\ 10^{-8}$
7	Bryan Mound (BM3C)	4.54	7623	0.268	2.22	0.594
8	Bryan Mound (BM4C)	5.18	8977	0.680	2.43	1.65
9	Bayou Choctaw (BC1)	4.06	5956	1.16	2.07	2.40
10	Etrez	3.1	4100	0.877	1.80	1.58
11	Avery Island (after S. and al.)	4.0	6565	5.53	2.05	11.3
12	Salina	4.1	8715	1.23	2.08	2.57
13	Palo Duro - Unit 4	5.6	9760	0.163	2.58	0.422
14	Palo Duro - Unit 5	5.3	9810	0.148	2.47	0.367
15	Asse (B.G.R.)	5.0	6495	0.663	2.37	1.57

Table 3: Steady-state convergence rate of a gas-filled spherical or cylindrical cavern opened to the atmosphere and located at a 1500 meters depth where the temperature is assumed to be 57°C (135°F). Gas pressure is 8 MPa.

Behavior of a closed tight cavern

If rock salt can be considered as absolutely impermeable (an arguable statement, and which be will discussed later) closure of a cavern will lead to pressure build-up: cavern convergence restrains the volume offered to brine, whose pressure increases accordingly. The increase is steeper when the cavern compressibility is small. A reasonable value for cavern compressibility (which encompasses both brine compressibility and cavern elasticity) is $\beta = 4\ 10^{-4}$ MPa^{-1}, which means that a $\dot{P}_i$ pressure rate is caused by a

$$-\dot{V}/V = \beta \dot{P}_i$$

relative volume loss rate ($\dot{V} < 0$) of the cavern. This value of β can vary to a large extent, especially when cavern shape is flat (in such a case, cavern creep is larger; a complete discussion makes use of F.E.M. calculations necessary). This relation can be combined with the two former relations which describe the relative volume loss rate of a spherical and cylindrical cavern; some straightforward algebra leads to:

$$P_\infty - P_i(t) = [P_\infty - P_i(0)]\,(1 + B\ t)^{\frac{-1}{n-1}}$$

where

$$\left|\begin{array}{ll} B_{sph} = \dfrac{3(n-1)A}{2\beta}\left(\dfrac{3}{2n}\right)^n \exp\left(-\dfrac{Q}{RT}\right)\ [P_\infty - P_i(0)]^{n-1} & \text{for a spherical cavern} \\ B_{cyl} = (2/\sqrt{3})^{(n+1)}\ B_{sph} & \text{for a cylindrical cavern} \end{array}\right.$$

Whether these steady-state relations apply for a cavern whose pressure is slowly modified by convergence is questionable, especially for relatively short periods of time after cavern closure. For we are mainly interested in long term behavior, when pressure rate becomes very small, these relations are considered as accurate enough.

From these steady-state formula, it is clear that the cavern pressure $P_i = P_i(t)$, which is initially equal to $P_i = P_i(0)$, slowly increases to the lithostatic value P_∞. Then frac risk must be discussed, as has been done by Wallner (1988), Wallner and Paar (1997).

On Figures 2 and 3 we considered the case of a cylindrical cavern at two different depths; first the cavern is 1000 meters deep ($T = 42°C$), then the cavern is 1500 meters deep ($T = 57°C$). When closing the cavern, the initial brine pressure $P_i(0)$ is equal to the weight of a brine-filled column (*Halmostatic pressure*).

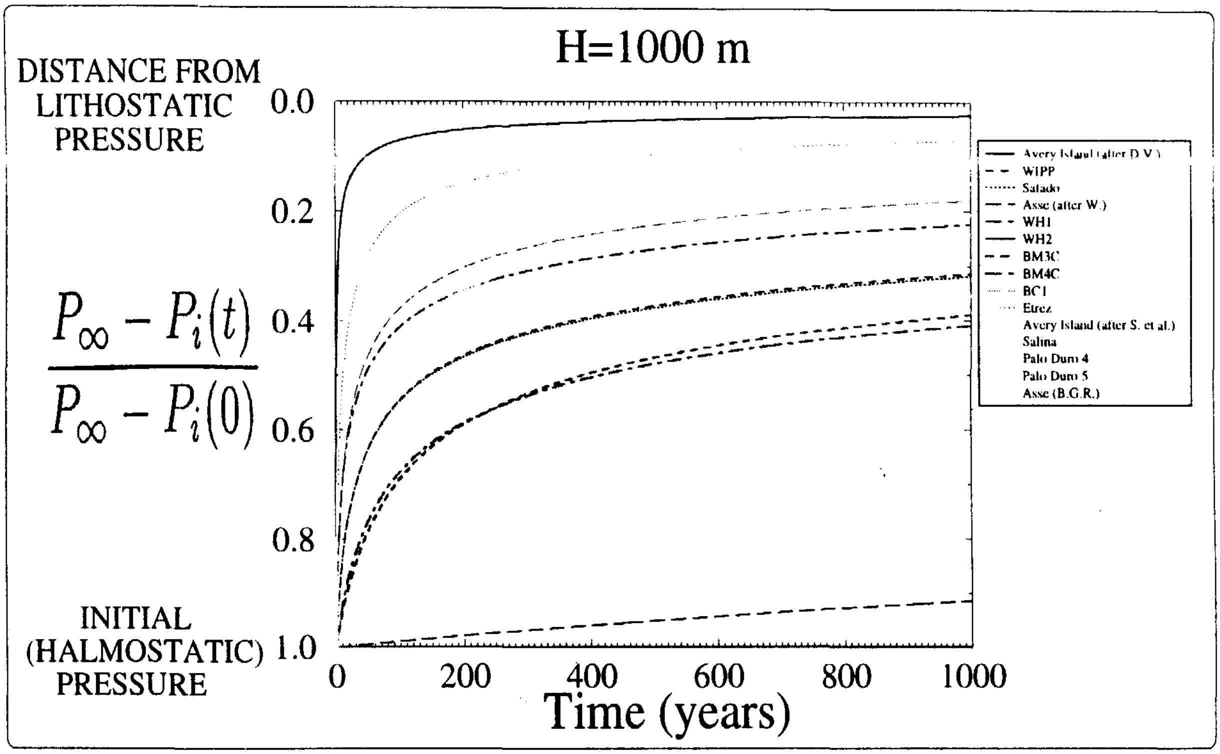

Figure 2: Cavern pressure build up after closure ($H = 1000$ m).

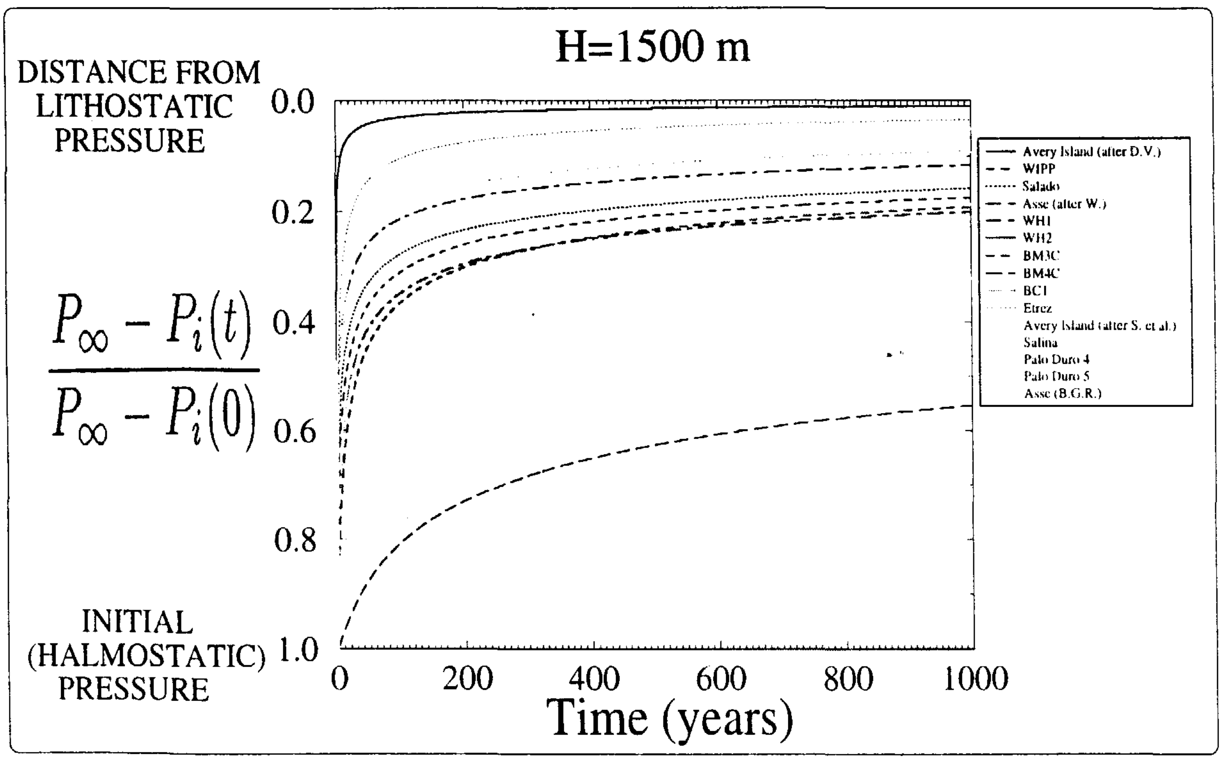

Figure 3: Cavern pressure build up after closure ($H = 1500$ m).

Behavior of a closed micropermeable cavern

These conclusions are deeply modified if a very small but non zero micropermeability of salt is taken into consideration, as has been discussed by Bérest (1990), Cosenza and Ghoreychi (1993), Bérest and Brouard (1995). We consider only in the following the case of a spherical cavern. The steady-state brine seepage from a cavern whose internal pressure is P_i, when the rock mass natural pore pressure is P_o, is easily calculated assuming Darcy's law:

$$\frac{Q}{V} = \frac{3K(P_i - P_o)}{\eta R^2}$$

where η is brine viscosity, R is cavern radius, and K is rock-salt intrinsic permeability.

When this brine percolation is taken into account, pressure build-up reaches much lower levels. An equilibrium will be reached when cavern loss of volume rate, due to creep, exactly balances the brine leakage flow, due to percolation toward the rock-mass:

$$\frac{3K(P_i - P_o)}{\eta R^2} = \frac{3}{2}\left[\frac{3}{2n}\left(P_\infty - P_i\right)\right]^n A \exp\left(-\frac{Q}{RT}\right)$$

We have calculated what would be the final equilibrium pressure when considering the former mechanical consitutive behaviors (See Figure 4 to 11). We have considered the case of a 1000 meters deep cavern ($P_\infty = 22$ MPa, $P_o = 12$ MPa, $T = 42$°C, $\eta = 1.2\ 10^{-3}$ Pa.s), and the case of a 1500 meters deep cavern ($P_\infty = 33$ MPa, $P_o = 18$ MPa, $T = 70$°C, $\eta = 1.0\ 10^{-3}$ Pa.s). A test (supported by SMRI) is currently in progress in a 930-meter deep cavern in the site of Etrez. The equilibrium pressure in the cavern seems to be 13 MPa (or 2 MPa at the well-head), which means that the in situ permeability is larger than 10^{-19} m^2. It must be noted that in most cases brine seepage rate is quite low.

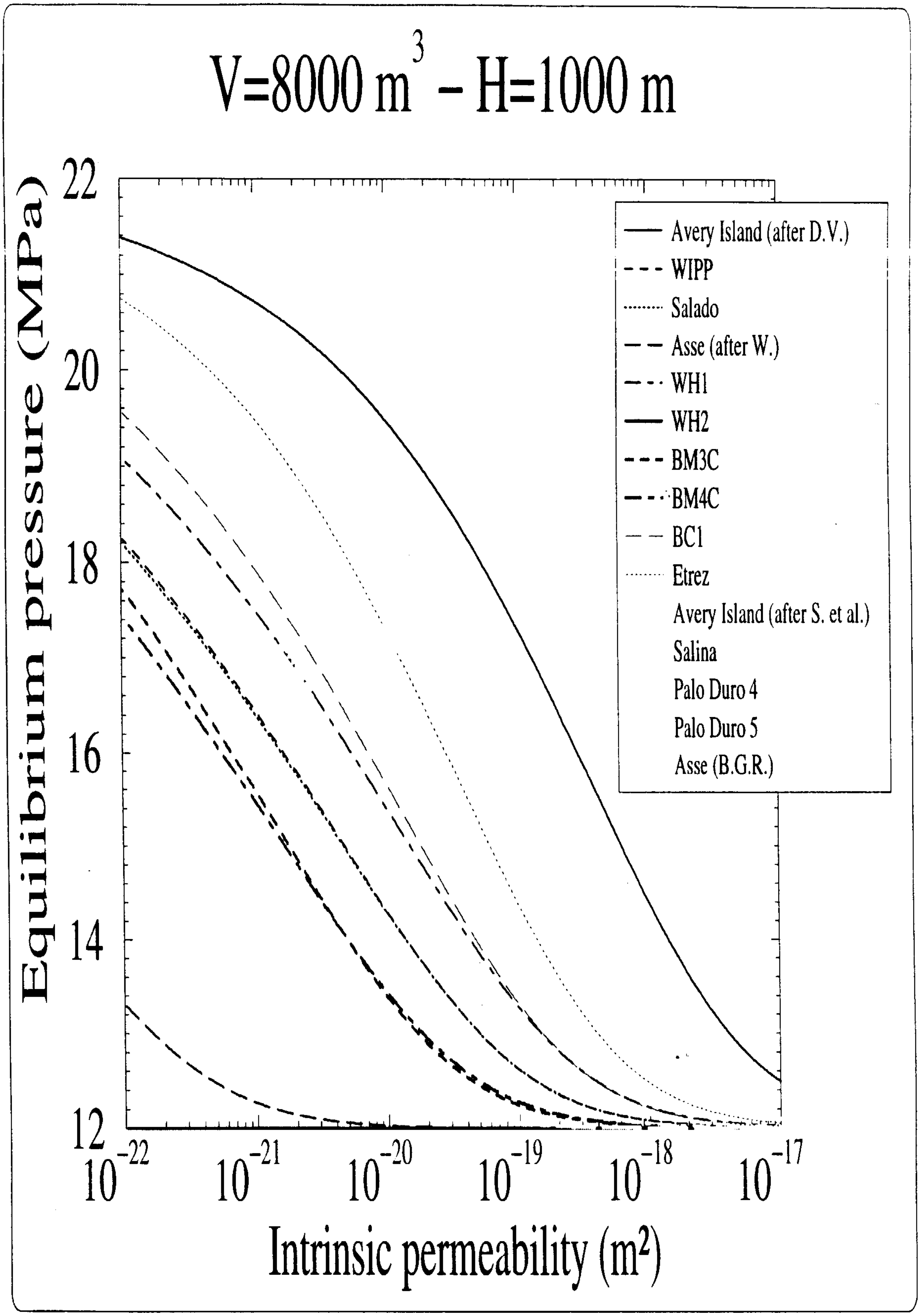

Figure 4: Equilibrium pressure versus intrinsic permeability ($V = 8000$ m^3, $H = 1000$ m).

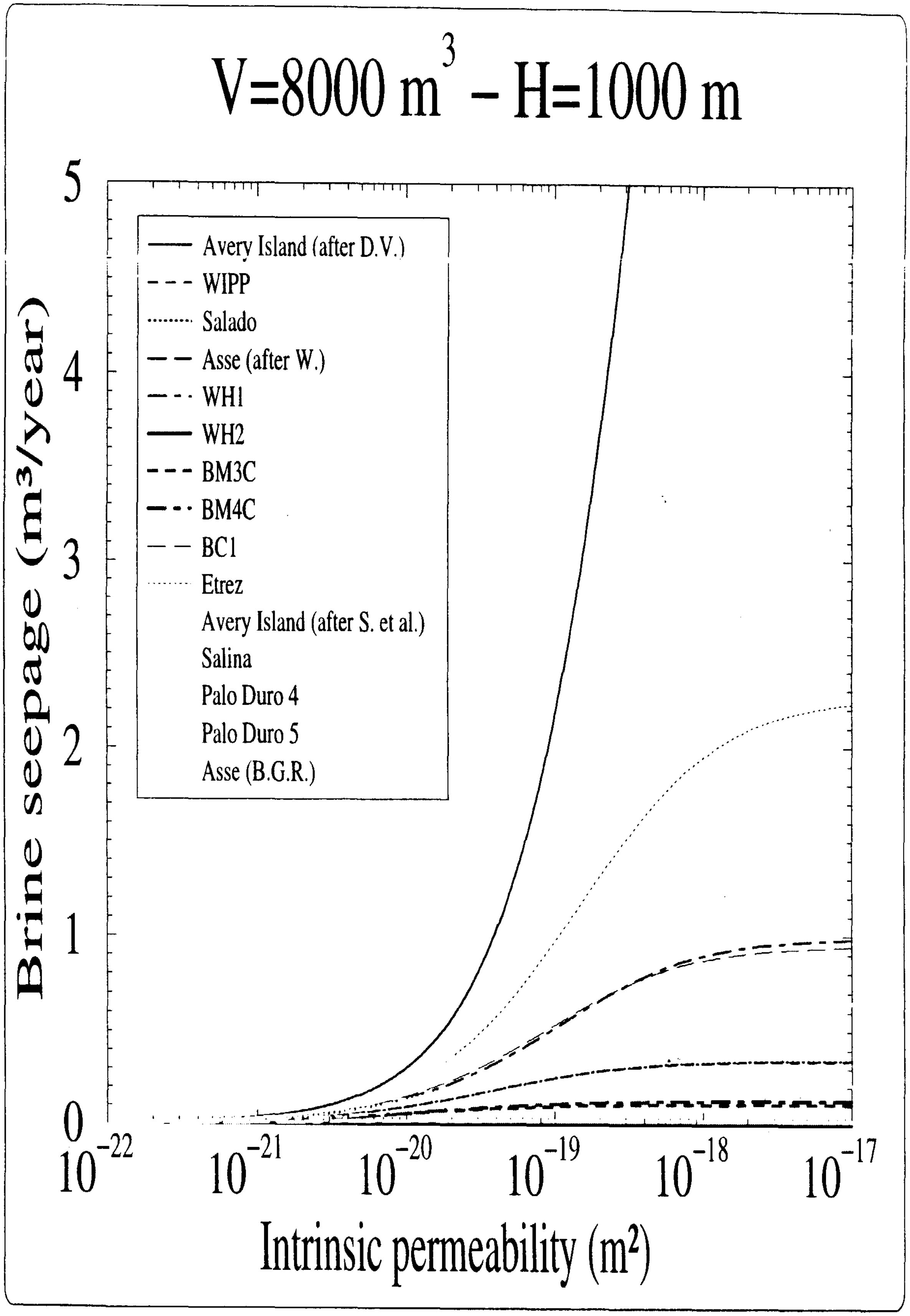

Figure 5: Brine seepage at equilibrium pressure ($V = 8000$ m^3, $H = 1000$ m).

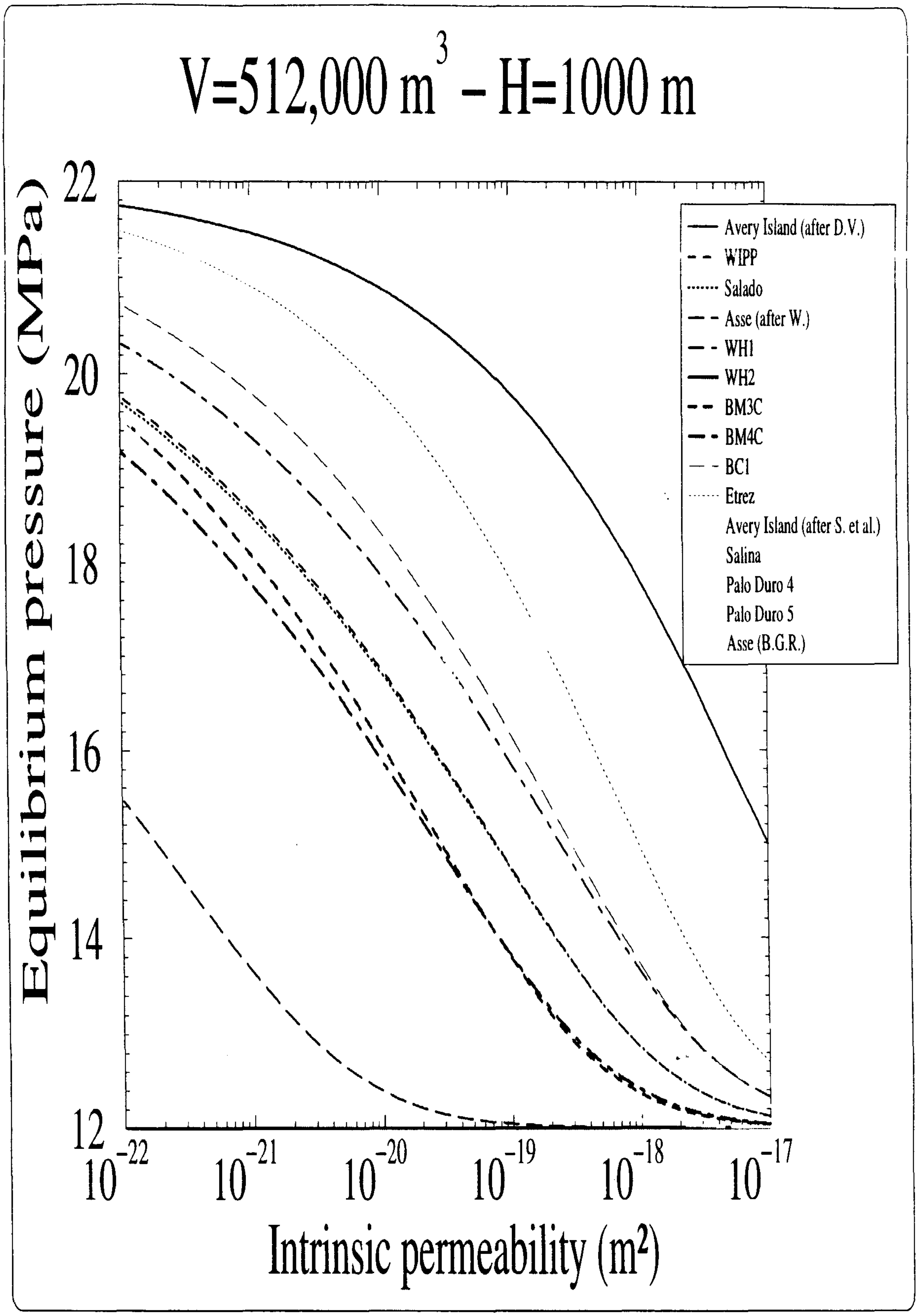

Figure 6: Equilibrium pressure versus intrinsic permeability ($V = 512,000\ \mathrm{m}^3$, $H = 1000$ m).

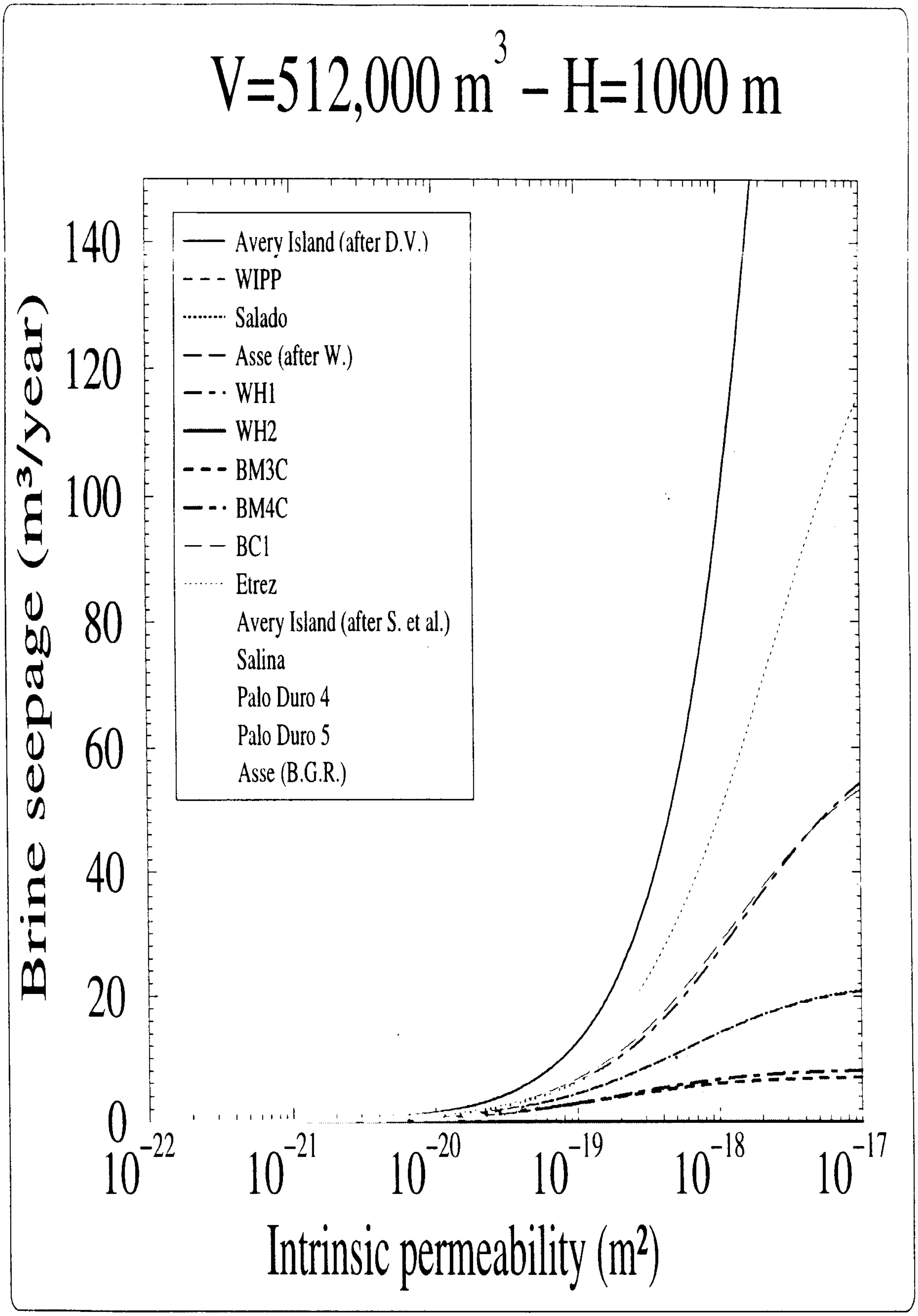

Figure 7: Brine seepage at equilibrium pressure ($V = 512,000$ m^3, $H = 1000$ m).

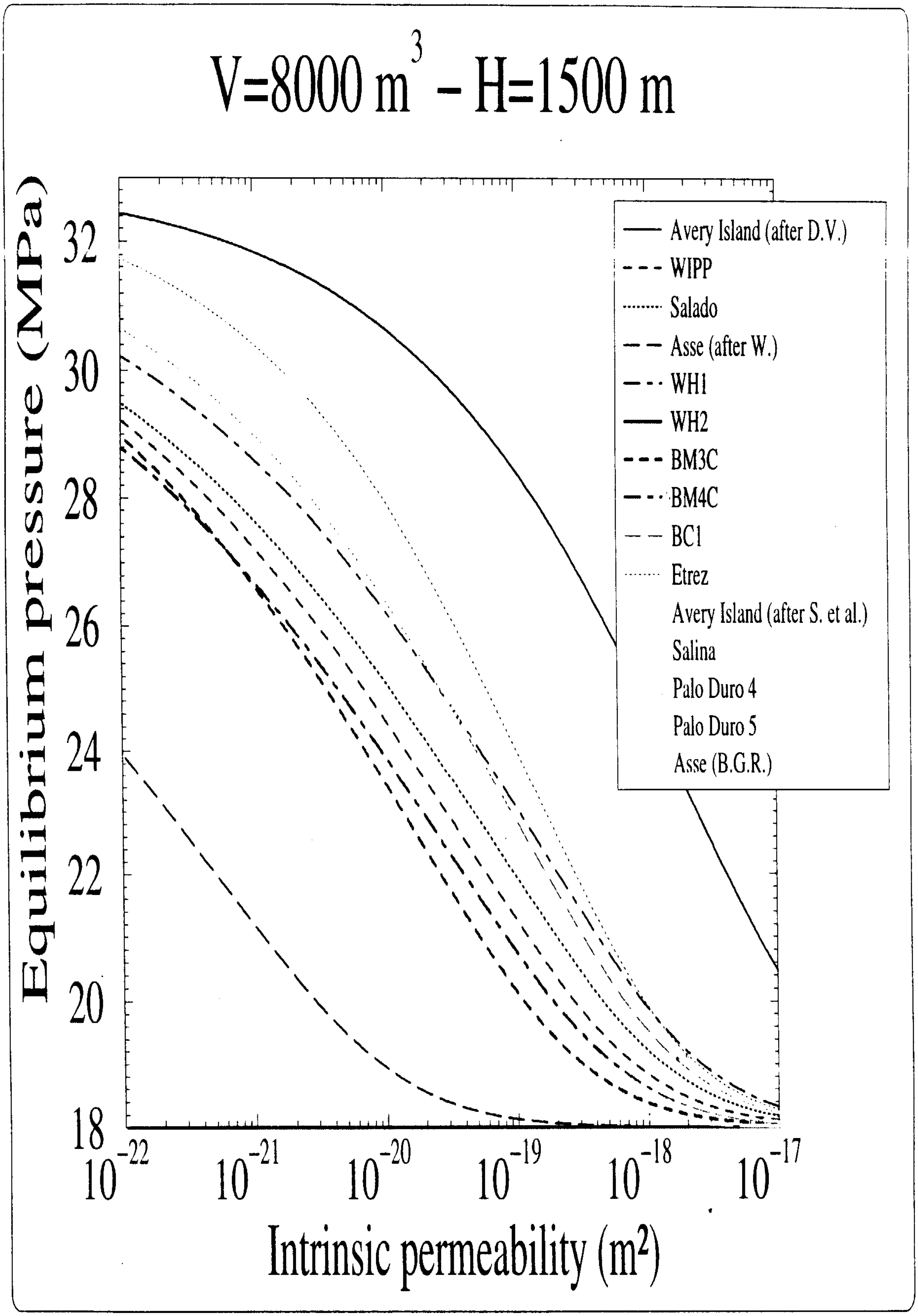

Figure 8: Equilibrium pressure versus intrinsic permeability ($V = 8000$ m^3, $H = 1500$ m).

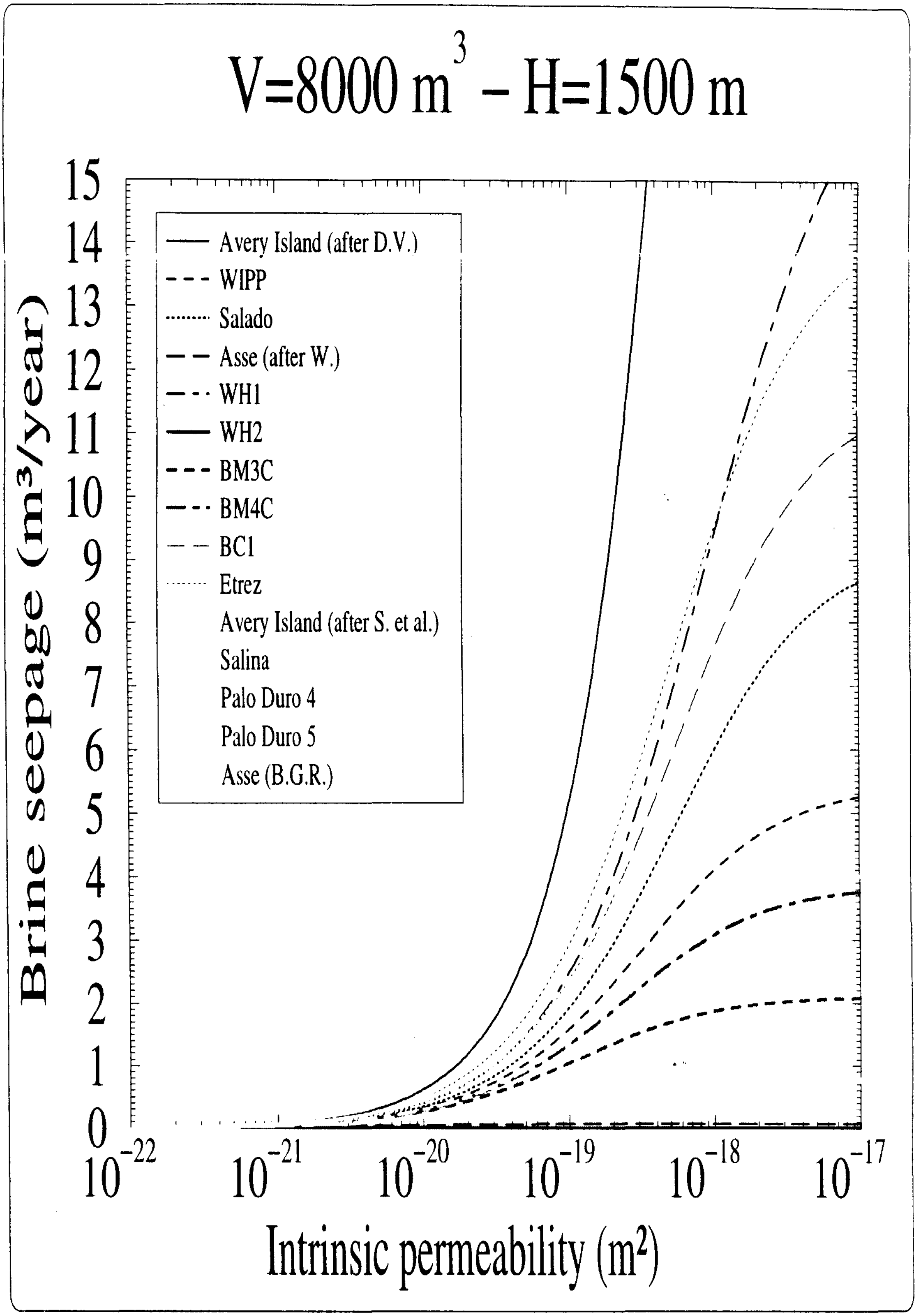

Figure 9: Brine seepage at equilibrium pressure ($V = 8000$ m^3, $H = 1500$ m).

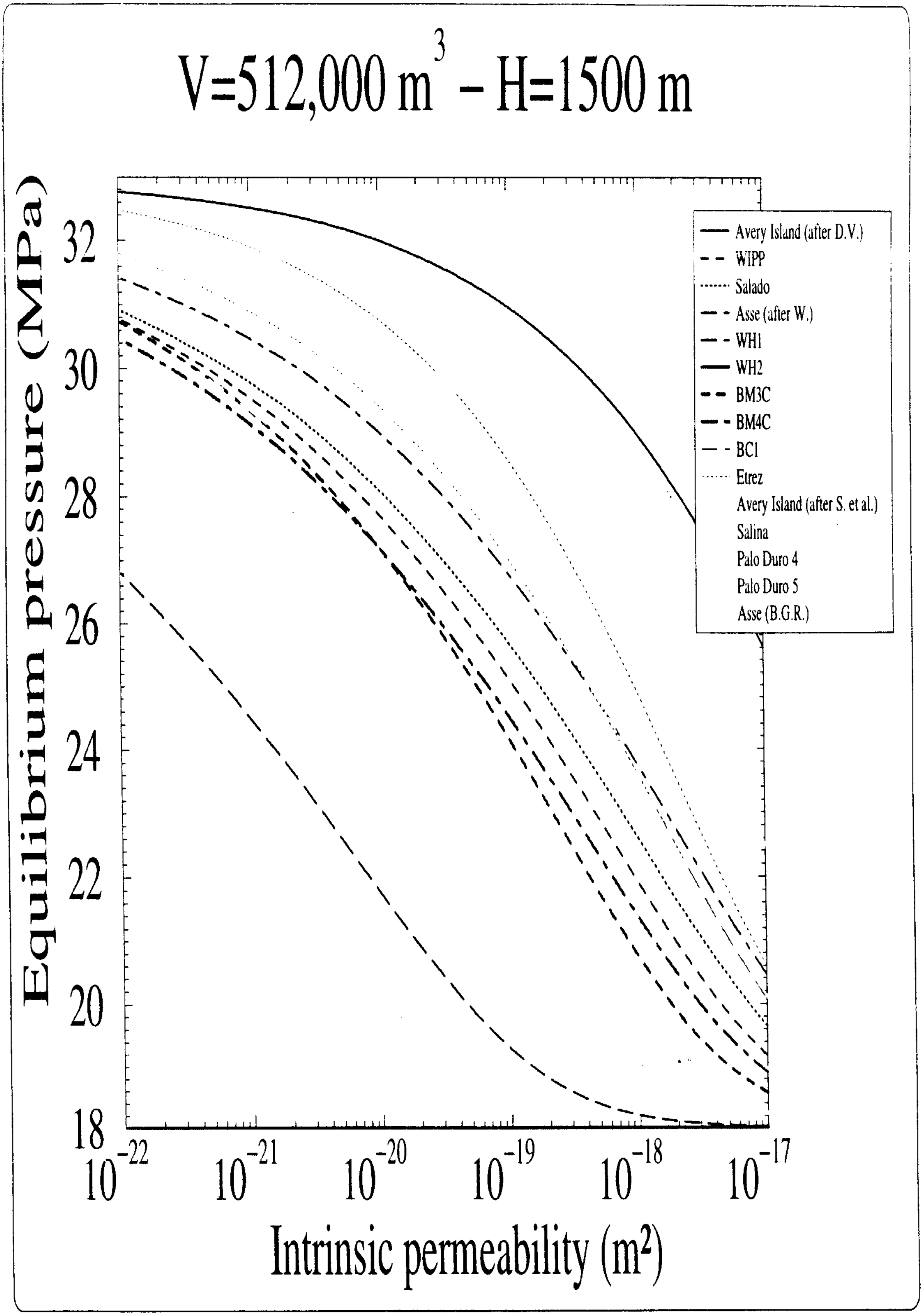

Figure 10: Equilibrium pressure versus intrinsic permeability ($V = 512,000$ m^3, $H = 1500$ m).

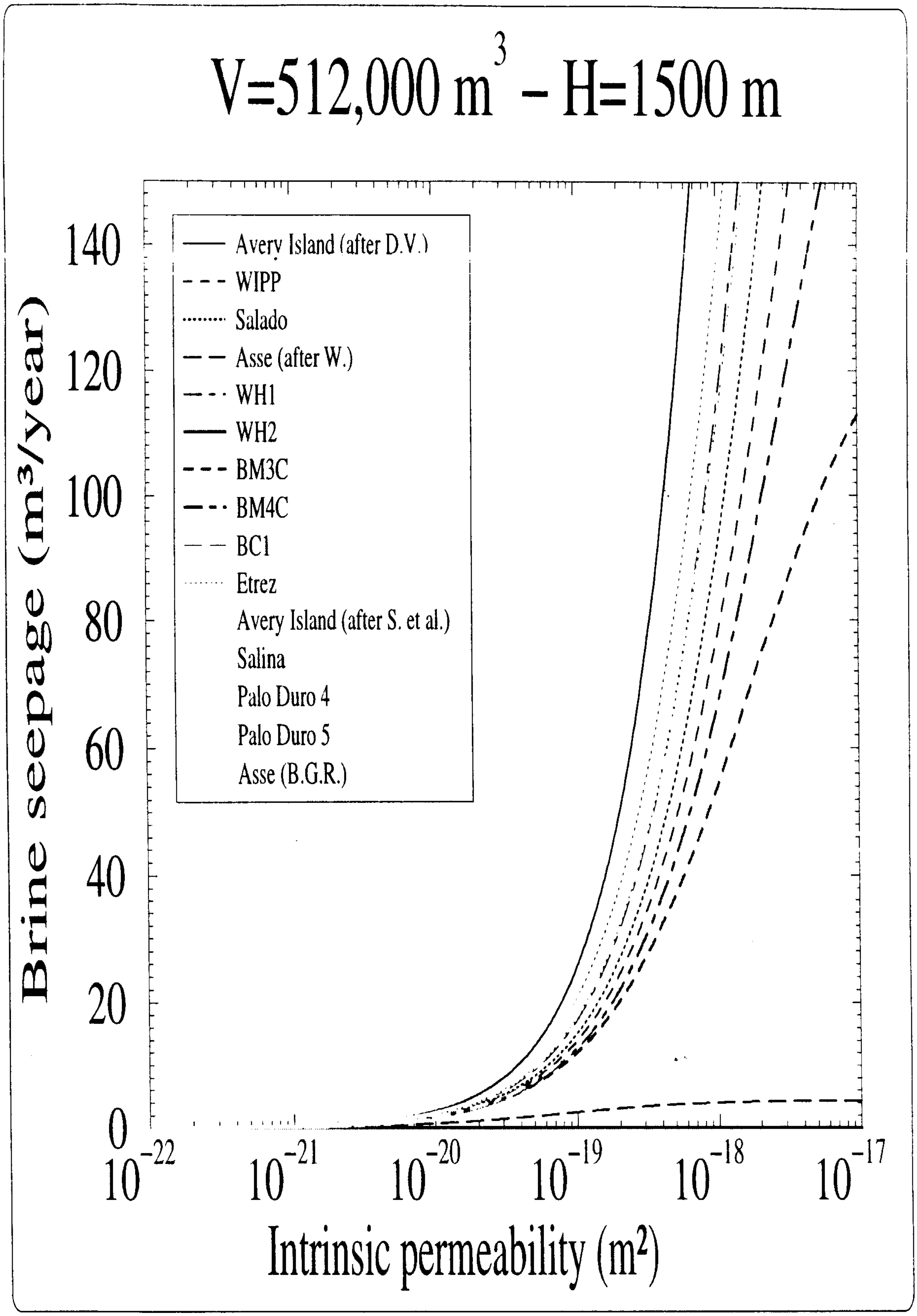

Figure 11: Brine seepage at equilibrium pressure ($V = 512,000 \text{ m}^3$, $H = 1500$ m).

Conclusions

1. Salt mechanical behavior is extremely complex. We have selected a standard power law which captures the main features of salt cavern behavior, at least when the cavern internal pressure slowly varies according to time. This law allows at least for rough estimations.

2. The set of selected parameters concerns 15 different constitutive laws found in the literature. These parameters are fitted on the results of laboratory tests that cover a range of deviatoric stresses well adapted to cavern creep problem and a range of temperatures poorly adapted to this problem. High temperatures (up to 200°C) are often taken into account, introducing a possible bias in cavern creep prediction.

3. The power law is generally expressed in the following form
$$\dot{\varepsilon} = A \exp\left(-\frac{Q}{RT}\right) \sigma^n$$
we suggest to use the following units: σ in MPa, Q/R in Kelvin, A in MPa^{-n}year^{-1}, which are convenient for application to storage caverns.

4. Using this system of units, we suggest computing the following quantity
$$\dot{\varepsilon}^{sph}_{1000} = \frac{3}{2}\left(\frac{3}{2n}\right)^n A\, P_o^n \exp\left(-\frac{Q}{RT_o}\right)$$
where $P_o = 10$ MPa, $T_o = 315$ K.
This quantity is the steady-state yearly loss of (relative) volume of a 1000-meter deep spherical cavern, when the cavern and the well are brine-filled and opened to the atmosphere.

5. The following classification is proposed

$\dot{\varepsilon}^{sph}_{1000} > 10^{-3}$ year^{-1}	severe creep can be expected
$\dot{\varepsilon}^{sph}_{1000} \approx 10^{-4}$ year^{-1}	standard salt
$\dot{\varepsilon}^{sph}_{1000} < 10^{-5}$ year^{-1}	low creep can be expected

6. This classification holds for a 1000-meter deep cavern. At larger depth, cavern creep is much larger. Large values of n and large value of Q favor increased creep at larger depth.

7. When available, in situ validation is of utmost importance. Prediction of long term behavior of underground caverns from laboratory tests is a difficult task, especially when caverns are deep and operating pressures are low.

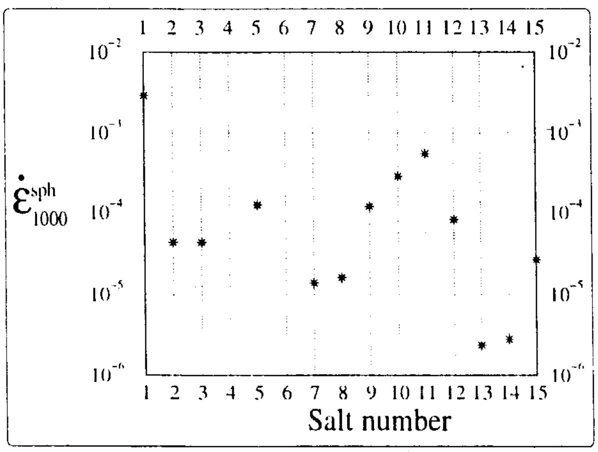

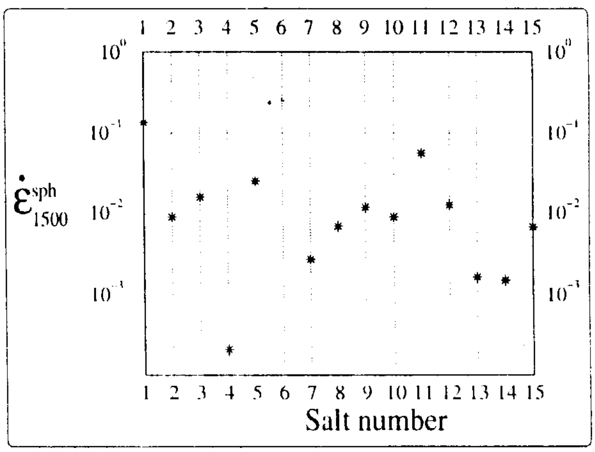

Figure 12: Yearly creep rate of a brine-filled spherical cavern at (H = 1000 m).

Figure 13: Yearly creep rate of a gas-filled spherical cavern at (H = 1500 m). Gas pressure is 8 MPa.

References

Hardy R.H. and Langer M., *Proc. 1st Conf. Mech. Beh. Salt*, 1984, Trans Tech Pub., Clausthal-Zellerfeld, 901 pages.

Hardy R.H. and Langer M., *Proc. 2nd Conf. Mech. Beh. Salt*, 1988, Trans Tech Pub., Clausthal-Zellerfeld, 781 pages.

Hardy R.H., Langer M., Bérest P. and Ghoreychi M., *Proc. 3rd Conf. Mech. Beh. Salt*, 1996, Trans Tech Pub., Clausthal-Zellerfeld, 621 pages.

Aubertin M., Hardy R.H., *Proc. 4th Conf. Mech. Beh. Salt*, 1998, Trans Tech Pub., Clausthal-Zellerfeld, 658 pages.

Brouard B., *On the behavior of solution-mined caverns* (in french), Ph.D. Thesis, 1998.

Baar C.A., *Applied Salt-Rock Mechanics, I*, Developments in Geotechnical Eng. 16-A, Elsevier, 1977.

Boucly P., *Expérience in situ et modélisation du comportement des cavités salines utilisées pour le stockage de gaz*, Revue française de Géotechnique, *n°* 18, pp.49-57, Février 1982.

Kuhne G., Rohr W.U., Sasse W., *Kiel gas storage facility, the first city gas cavern in Germany*, Proc. 12th World Gas Congress, Nice, 1973.

Bérest P., Brouard B., Durup G., *Behavior of Sealed solution-mined caverns*, Proc. 4th Conf. Beh. of Salt, Aubertin and Hardy ed., Trans Tech Pub., Clausthal-Zellerfeld, pp.511-524, 1998.

Pouya A., *Correlation between mechanical behavior and petrological properties of rock salt*, Proc. 32th US Rock Mech. Symp., J.C. Roegiers ed., pp.385-392, 1991.

Van Sambeek L.L., *Evaluating Cavern Tests and Subsurface Subsidence Using Simple Numerical Models*, 7th Symp. on Salt, Elsevier, Amsterdam, Vol. I, pp.433-439, 1993.

De Vries K.L., *Viscoplastic Laws for Avery Island Salt*, RE/SPEC Inc. Report prepared for Stone and Webster Engineering Corporation (quoted by Van Sambeek, 1993), 1988.

Munson D.E., Fossum A.F., Senseny P.E., *Approach to First Principles model prediction of measured WIPP in situ closure in salt*, Proc. 30th US Rock Mech. Symp., A Wahab Khair ed., pp.673-680 (quoted by Van Sambeek, 1993), 1989.

Senseny P.E., *Creep properties of four rock salts*, Proc. 2nd Conf. Mech. Beh. of Salt, Hardy and Langer ed., Trans Tech Pub., pp.431-444, 1984.

Wawersik W.R., *Alternatives to a power-law creep model for rock salt at temperatures below 160°C*, Proc. 2nd Conf. Mech. Beh. of Salt, Hardy and Langer ed., Trans Tech Pub., Clausthal-Zellerfeld, pp.103-128, 1984.

Heusermann S., *Measurements of initial rock stress at the Asse Salt Mine*, Proc. 3rd Conf. Mech. Beh. of Salt, Ghoreychi, Bérest, Hardy and Langer ed., Trans Tech Pub., Clausthal-Zellerfeld, pp.101-114, 1996.

Prij J., *On the design of a radioactive waste repository*, Ph.D. Thesis, Twente University, 1991.

Bérest P., Brouard B., Bergues J., Frelat J., Durup G., *Salt Caverns and the Compressibility Factor*, SMRI Fall Meeting, El Paso, 1997.

Wallner M., *Frac pressure risk for cavities in rock salt*, 2nd Conf. Mech. Beh. of Salt, Hardy and Langer ed., Trans Tech Pub., Clausthal-Zellerfeld, pp.645-658, 1988.

Wallner M., Paar W., *Risk of Progressive Pressure Build up in a Sealed Cavity*, SMRI Fall Meeting, El Paso, 1997.

Bérest P., Brouard B., *Salt Cavern Abandonment* (in french), Revue française de Géotechnique, to be published in 1998.